Dalton Transactions

PAPER

View Article Online
View Journal

Cite this: DOI: 10.1039/c4dt01206b

Scandium *versus* yttrium{amino-alkoxy-bis-(phenolate)} complexes for the stereoselective ring-opening polymerization of racemic lactide and β-butyrolactone†

Yulia Chapurina,[a] Joice Klitzke,[a,b] Osvaldo de L. Casagrande Jr.,[b] Mouhamad Awada,[a] Vincent Dorcet,[c] Evgueni Kirillov*[a] and Jean-François Carpentier*[a]

Received 24th April 2014,
Accepted 13th May 2014

DOI: 10.1039/c4dt01206b

www.rsc.org/dalton

Scandium and yttrium amide complexes Ln{ONXO^{R1,R2}}(N(SiHMe$_2$)$_2$)(THF)$_n$ (Ln = Sc, n = 0 or Y, n = 1; X = NMe$_2$ or OMe; R^1 = Cumyl or p-Cl-Cumyl; R^2 = Me or Cumyl) were prepared by aminolysis of Ln[N(SiHMe$_2$)$_2$]$_3$(THF) with the corresponding tetradentate diamino- or alkoxy-amino-bis(phenol) pro-ligands {ONXO^{R1,R2}}H$_2$. In the solid state and in toluene solution, the scandium complexes are monomeric and 5-coordinated, while the analogous yttrium complexes all bear an extra THF-coordinated molecule and are 6-coordinated. Sc{ONXO^{R1,R2}}(N(SiHMe$_2$)$_2$) complexes are single-site initiators for the ring-opening polymerization (ROP) of racemic lactide but are less active than their yttrium analogues Y{ONXO^{R1,R2}}-(N(SiHMe$_2$)$_2$)(THF); also, in contrast to the latter ones, they are inactive in the ROP of the more demanding racemic β-butyrolactone. On the other hand, the scandium amide complexes feature a significantly improved control over the ROP of lactide, yielding PLAs with much narrower molecular weight distributions ($Đ_M$ < 1.1 for Sc *vs.* 1.5–2.0 for Y). The yttrium complex with the very bulky *o*,*p*-dicumyl-substituted ligand is more heteroselective than its scandium analogue (P_r = 0.88 *vs.* 0.83), while the opposite is observed with complexes based on *p*-methyl-substituted ligands (P_r = 0.50 in toluene or 0.72–0.75 in THF for Y *vs.* P_r = 0.75–0.83 for Sc in toluene). These reactivity and selectivity trends are rationalized by a much more sterically crowded coordination sphere in scandium than in yttrium complexes.

Introduction

The ring-opening polymerization (ROP) of cyclic esters such as the ubiquitous lactide but also the more demanding β-lactones is a highly topical research field due to the renewability of some of these monomers and the biocompatibility and valuable properties of the corresponding polymers.[1] Extensive research over the past 15 years has demonstrated that rare earth complexes supported by multidentate bis(phenolate) type ligands are extremely efficient catalysts/initiators for the controlled ROP of such cyclic esters.[2] In particular, yttrium complexes with dianionic, tetradentate amino-bridged bis(phenolate) ancillary ligands {ONXO}$^{2-}$ having an additional alkoxy or amino X cap (**A**, Fig. 1) have appeared as a unique class of catalysts due to their very high activity, living character, but also

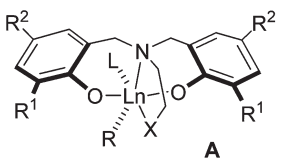

A

Ln = rare earth/lanthanide
R = alkyl, amide, alkoxide
X = OMe, NMe$_2$, pyridyl...
R^1, R^2 = alkyl, halogen...
L = THF, pyridine... or none

Fig. 1 Rare earth complexes supported by tetradentate {ONXO}$^{2-}$ ancillary ligands.

[a]*Institut des Sciences Chimiques de Rennes, Organometallics: Materials and Catalysis Laboratories, UMR 6226 CNRS-Université de Rennes 1, F-35042 Rennes Cedex, France. E-mail: evgueni.kirillov@univ-rennes1.fr, jean-francois.carpentier@univ-rennes1.fr*

[b]*Instituto de Química, Laboratório de Catálise Molecular, Universidade Federal do Rio Grande do Sul, Av. Bento Gonçalves, 9500, Porto Alegre, RS 90501-970, Brazil*

[c]*Institut des Sciences Chimiques de Rennes, Centre de diffraction X, UMR 6226 CNRS-Université de Rennes 1, F-35042 Rennes Cedex, France*

†Electronic supplementary information (ESI) available: X-ray crystallographic data for pro-ligands **L1**, **L2**, and **L3** and complexes **Sc-1**, **Sc-3**, **Sc-4**, and **Y-2** as CIF files; the molecular structure of pro-ligands **L1**, **L2**, and **L3** and complexes **Sc-1**, **Sc-3**, **Sc-4**, and **Y-2**; ^{1}H and ^{13}C{^{1}H} NMR spectra of the prepared pro-ligands and complexes. CCDC 1002394–1002400. For ESI and crystallographic data in CIF or other electronic format see DOI: 10.1039/c4dt01206b

even more because of their capacity to fine control the stereoselectivity of the ROP when starting from racemic mixtures of chiral cyclic esters.[3] Highly heterotactic polylactide (PLA) and highly syndiotactic poly(β-hydroxyalkanoate)s[4] were thus respectively prepared from racemic lactide (*rac*-LA) and β-lactones such as β-butyrolactone (*rac*-BL) and substituted analogues.

The stereoselectivity in those coordination–insertion polymerizations mediated by nonchiral catalysts originates from a so-called chain-end control, in which the stereoselection of the incoming monomer unit depends on the chirality of the last inserted monomer unit in the growing polymer chain. It is generally acknowledged that chain-end control is favored by a sterically congested environment at the active metal center, so that the chirality of the growing polymer chain can effectively exert a selection between enantiomers of the monomer.[1] Hence, it is not surprising to see that the most effective catalysts of type A for achieving stereocontrolled ROP have very bulky substituents at the *ortho* position of the phenolate rings, namely *tert*-butyl or even better adamantyl, and especially cumyl and trityl groups.[3,4b,c,5] Similarly, small metal centers are preferred because, once enwrapped by the $\{ONXO\}^{2-}$ ligand, they leave little space for the growing polymer chain and coordination of the incoming monomer. Yttrium and lutetium have hence demonstrated clearly superior stereocontrol abilities than the (much) larger rare earths (Sm, Nd, La, *etc.*).[6] Surprisingly enough, there are very few examples of complexes of the small[7] scandium supported by the $\{ONXO\}^{2-}$ ligand,[8] and none of them was used in ROP. More generally, examples of scandium complexes in stereoselective ROP reactions are quite limited.[6a,f,i,j,o,9]

Herein, we report on the preparation and structural characterization of a series of Sc{ONXO} amide complexes. The $\{ONXO\}^{2-}$ ligands for this study have been selected based on the aforementioned trends, for a potentially high stereocontrol in ROP of *rac*-LA and *rac*-BL and an optimal comparison of the catalytic performance of the scandium complexes with their yttrium analogues. The coordination chemistries of these two families of complexes are also compared.

Results and discussion

Pro-ligands

To explore the steric and possible electronic influence of substituents on the phenolate rings and side arms on stereoselective ROP, a set of four pro-ligands was targeted (Scheme 1). Those pro-ligands were selected to afford direct comparisons with reference yttrium systems that have proven to offer some of the best catalytic performances thus far in ROP of *rac*-LA and *rac*-BL,[3b,4b,c] that is, the methoxy-amino-bis(phenolate) system bearing *ortho*,*para*-cumyl substituents derived from $\{ONOO^{Cum,Cum}\}H_2$ (**L4**). In addition, the new pro-ligands $\{ONNO^{Cum,Me}\}H_2$ (**L1**), $\{ONOO^{Cum,Me}\}H_2$ (**L2**) and $\{ONOO^{CumCl,Me}\}H_2$ (**L3**) bearing respectively an *N*,*N*-dimethylamino cap in place of the methoxy cap, and a cumyl or a *p*-chloro-substituted cumyl group, to explore potential electronic effects such as in the *p*-CF_3-substituted cumyl compounds,[4c] were prepared. Compounds **L1**, **L2** and **L3** were synthesized by a regular double Mannich condensation of the corresponding substituted phenol, formaldehyde, and diamine or methoxyamine in methanol, and isolated in 36–90% yield after recrystallization as white microcrystalline powders. They were authenticated by elemental analysis, ^1H, $^{13}C\{^1H\}$ NMR spectroscopy (see the Experimental section), and X-ray diffraction studies (see the ESI†).

Synthesis and solution structure of scandium- and yttrium-amide complexes

Heteroleptic scandium-$\{ONXO^{R1,R2}\}$ amide complexes were prepared straightforwardly by amine elimination reaction from $Sc[N(SiHMe_2)_2]_3(THF)$ and one equivalent of the corresponding

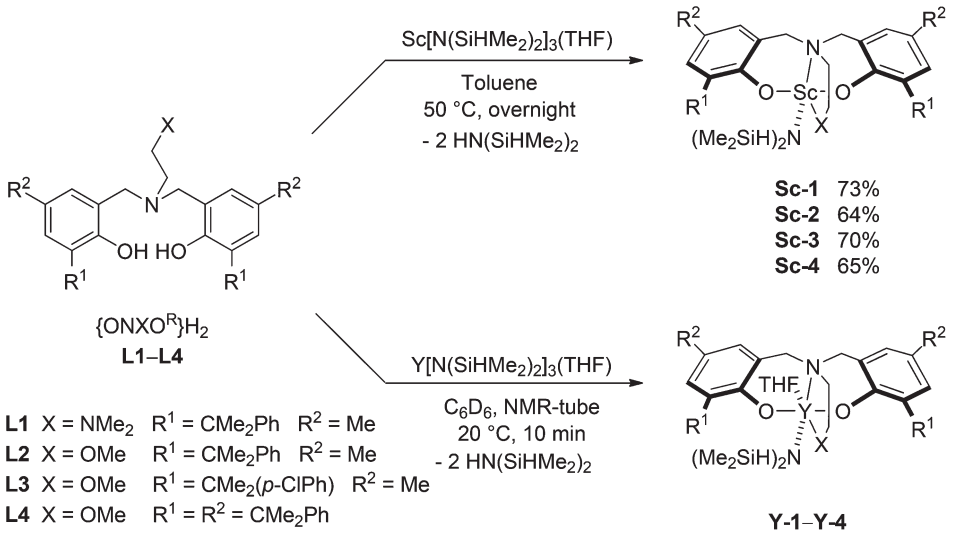

Scheme 1 Synthesis of scandium- and yttrium-$\{ONXO^{R1,R2}\}$ amide complexes.

pro-ligands {ONXO^{R1,R2}}H$_2$ at 50 °C (Scheme 1). Complexes **Sc-1–Sc-4** were isolated in 64–73% yields as white solids, which are air- and moisture-sensitive and readily soluble in most usual organic solvents. The structure of these complexes was established on the basis of ^{1}H, ^{13}C{^{1}H}, ^{29}Si and ^{29}Si{^{1}H} NMR spectroscopy in solution, elemental analysis, and single-crystal X-ray diffraction studies for **Sc-1**, **Sc-3**, and **Sc-4**.

As for their previously reported analogue **Y-4**,[3b,4b,c] the new yttrium complexes **Y-1**, **Y-2** and **Y-3** were also synthesized by direct aminolysis of Y[N(SiHMe$_2$)$_2$]$_3$(THF) with the corresponding pro-ligands **L1–L3**. The reactions proceeded cleanly in benzene-d_6, at room temperature, as evidenced by NMR monitoring. However, as mentioned earlier,[4b,c] the preparation of these compounds on a larger scale, in toluene at room temperature, and their eventual isolation was found to be more complicated. A mixture of the desired complex contaminated with 5–10% of an unidentified species was often observed, and complete purification could not be achieved. For that reason, complexes **Y-1**, **Y-2** and **Y-3** were conveniently generated *in situ* for further use in catalysis, but were not isolated.

The ^{1}H and ^{13}C{^{1}H} NMR data for **Sc-1** in benzene-d_6 at 338 K, and for **Sc-2** and **Sc-3** in benzene-d_6 at room temperature contain all single sets of sharp resonances that are consistent with monomeric species in solution,[6o] with a rigid C_s symmetry. Both methyl groups of the silylamide group SiH*Me*$_2$ are equivalent on the NMR timescale and only one multiplet is observed for the Si*H*Me$_2$; also, in the ^{29}Si{^{1}H} and ^{29}Si NMR spectra of **Sc-1** and **Sc-3**, the silylamide groups appear as a sharp singlet and a doublet of multiplets ($^1J_{Si-H}$ = *ca.* 162–172 Hz, $^2J_{Si-H}$ = *ca.* 6.5–7.1 Hz, see the ESI†), respectively, evidencing the equivalence of the Si atoms. The ^{1}H resonances for the capping X group appear at δ 1.64 (for the NMe$_2$ group in **Sc-1**) and δ 2.79 and 2.90 ppm (for the OMe group in **Sc-2** and **Sc-3**), shifted by approximately 0.3–0.6 ppm upfield with respect to that in the pro-ligand; this indicates that this X (N, O) group remains coordinated in solution onto the metal center, which is thus 5-coordinated. This assignment of solution structures of scandium compounds was supported by single-crystal X-ray structure analyses of **Sc-1**, **Sc-3** and **Sc-4** (*vide infra*).

In contrast, the NMR spectra of **Sc-4** in benzene-d_6 are quite broad at room temperature, and heating at 333 K was necessary to sharpen significantly the resonances. Relevant ^{1}H NMR data at this temperature include two distinct multiplets for the Si*H*Me$_2$ hydrogens (δ 4.87 and 5.01 ppm), and one sharp doublet and one broadened doublet for the SiH*Me*$_2$ groups (δ 0.29 and 0.33 ppm), each of equal intensity, respectively. Also, two signals for the SiH*Me*$_2$ groups are also observed in the ^{13}C{^{1}H} NMR spectrum, while two distinct (one sharp and one broadened), equal intensity resonances are observed in the ^{29}Si{^{1}H} NMR spectrum (δ −20.4 and −20.3 ppm; see the ESI†). These observations evidence that **Sc-4** adopts a non-symmetric structure in solution at this temperature. Since **Sc-4** is monomeric in the solid state (*vide infra*) and since such features are not observed in the NMR spectra of **Sc-2** and **Sc-3**, we assume that this dissymmetry of **Sc-4** in solution originates from the combined steric crowding between the bulky *ortho*- and *para*-cumyl substituents.

In contrast to the scandium complexes, a coordinated THF molecule was systematically observed by ^{1}H and ^{13}C NMR spectroscopy in yttrium complexes **Y-1**, **Y-2** and **Y-3**, as evidenced by THF resonances clearly shifted from those of the free solvent (δ(^{1}H) 1.40 and 3.57 ppm; δ(^{13}C) 25.72 and 67.80 ppm in benzene-d_6). This observation, which is in line with the solid-state structure of **Y-2** (*vide infra*) and with previous observations made on related rare earth complexes of the type Ln{ONXO^{R1,R2}}(N(SiHMe$_2$)$_2$)(THF),[3,4] indicates that **Y-1–Y-3** are mononuclear and six-coordinated in benzene or toluene solution. The chemical shifts for the Si*H*Me$_2$ resonance (δ 4.68–4.80 ppm in benzene-d_6), which are shifted upfield compared to the chemical shift in the corresponding Y[N(SiHMe$_2$)$_2$]$_3$(THF) precursor, argue against a strong β(Si–H) agostic interaction with the metal center in solution.

Solid-state structure of scandium- and yttrium-amide complexes

Crystals suitable for X-ray diffraction studies were grown at room temperature from a concentrated heptane solution for **Sc-1** and from toluene–hexane solutions for **Sc-3**, **Sc-4** and **Y-2**. The solid-state molecular structures of these complexes are shown in Fig. 2–5. The main crystallographic details are reported in Tables S3 and S4 of the ESI.† Selected bond distances and angles for these compounds are given in Table 1.

All three scandium complexes exhibited essentially the same geometry, that is, a five-coordinated metal center in a distorted square-based pyramidal (*sbp*) environment; one O(phenolate) atom of the {ONXO^{R1,R2}}$^{2-}$ ligand occupies the axial position and the three other heteroatoms (O, N, and X) of the ligand and the N(amide) form the square basis (trigonal index, τ = 0.17 (**Sc-1**); 0.00 (**Sc-3**), 0.02 (**Sc-4**)),[10] the metal lying *ca.* 0.5 Å above the square basis (0.51, 0.49 and 0.45 Å, respectively). This five-coordinated *sbp* geometry[11] contrasts with the six-coordinated (distorted) octahedral geometry observed in

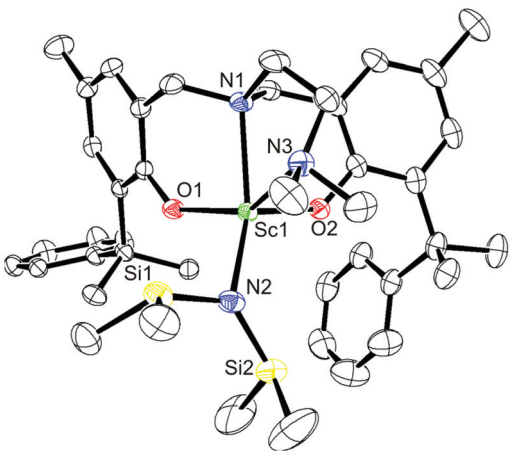

Fig. 2 Solid-state molecular structure of Sc{ONNO^{Cum,Me}}(N(SiHMe$_2$)$_2$) (**Sc-1**). All hydrogen atoms are omitted for clarity; thermal ellipsoids are drawn at the 50% probability level.

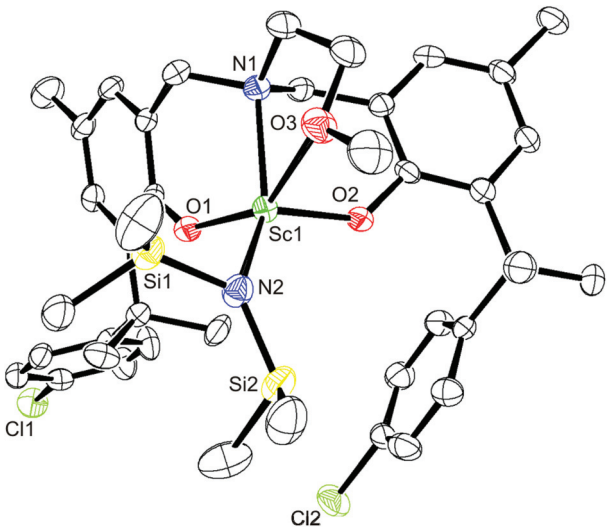

Fig. 3 Solid-state molecular structure of Sc{ONOO^{CumCl,Me}}-(N(SiHMe$_2$)$_2$) (**Sc-3**). All hydrogen atoms are omitted for clarity; thermal ellipsoids are drawn at the 50% probability level.

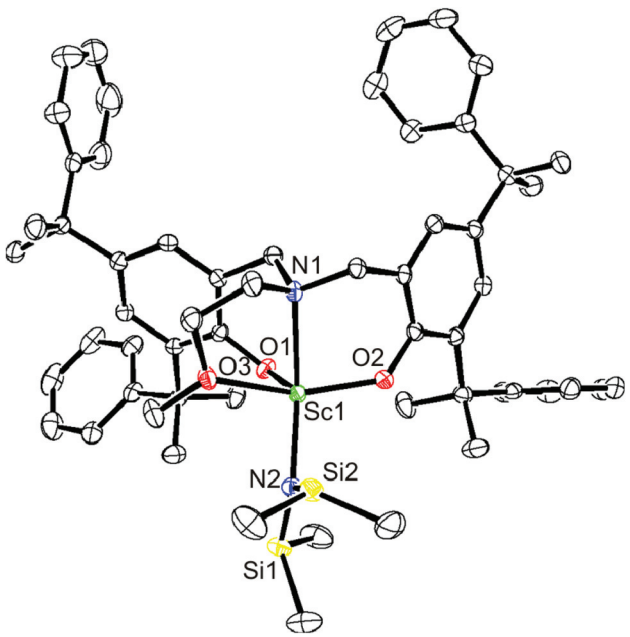

Fig. 4 Solid-state molecular structure of Sc{ONOO^{Cum,Cum}}-(N(SiHMe$_2$)$_2$) (**Sc-4**). All hydrogen atoms are omitted for clarity; thermal ellipsoids are drawn at the 50% probability level.

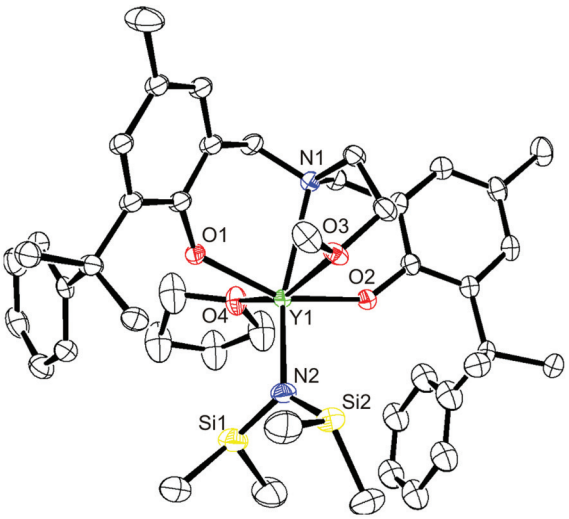

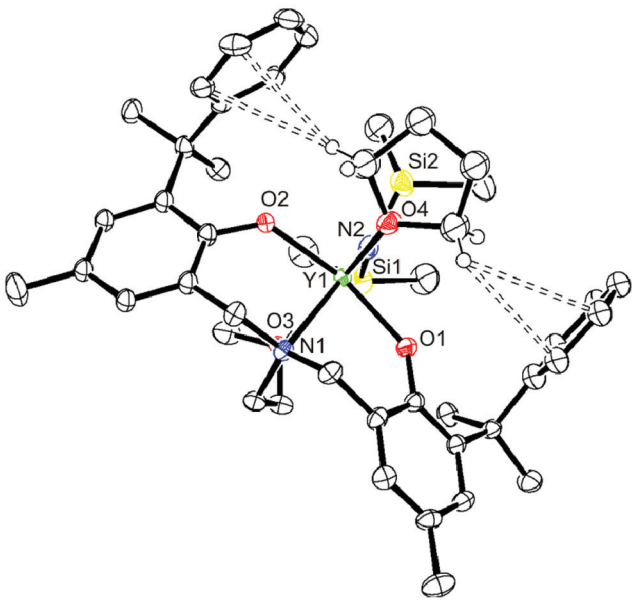

Fig. 5 Solid-state molecular structure of Y{ONOO^{Cum,Me}}(N(SiHMe$_2$)$_2$)-(THF) (**Y-2**). Thermal ellipsoids are drawn at the 50% probability level. In the top view, all hydrogen atoms are omitted for clarity. The bottom view shows the parallel orientation of the phenyl cumyl rings along the N(amido)–Y–O(THF) plane, with the (THF)C–H···π(phenyl) close contacts.

Mountford's monomeric Sc{ONNO^{tBu,tBu}}Cl(pyridine) and dimeric phenoxy-bridged [Sc{ONNO^{Me,Me}}Cl]$_2$;[8] obviously, the steric hindrance induced by the bulky cumyl substituents prevents such dimerization in **Sc-1**, **Sc-3** and **Sc-4**. The Sc–O (phenolate) bond lengths (1.947(2)–1.969(1) Å) are in the normal range of values found in related Sc-phenolate compounds.[8,9] The bond angles involving the oxygen phenolate atoms (O(1)–Sc(1)–O(2), 104.3(5)–107.34(5)°) and the *trans*-located nitrogen atoms of the bridging amine and amide ligands (N(1)–Sc(1)–N(2), 149.07(8)–154.76(6)°) are quite similar. The Sc–O(methoxy) bond lengths in **Sc-3** and **Sc-4** (Sc(1)–O(3), 2.268(2) and 2.249(1) Å) are expectedly shorter than the Sc–N(capping amine) bonds in **Sc-1** (Sc(1)–N(3), 2.411(2) Å); the latter bond appears longer than that observed (2.303(6) Å) for the corresponding Sc–N(capping 2-pyridyl) in the 6-coordinate Sc{ONNO^{tBu,tBu}}Cl(pyridine),[8] forming a similar 5-metallacycle. The Sc–N(bridging amine) bonds (Sc(1)–N(1), 2.320(2)–2.341(1) Å) compare well with that observed in Sc{ONNO^{tBu,tBu}}Cl(pyridine) (2.387(2) Å)[8] and are expectedly *ca.* 0.2 Å longer than the Sc–N(amide) bonds (Sc(1)–N(2), 2.089(1)–2.109(2) Å). All those M–N/O bond distances are *ca.* 0.2–0.3 Å shorter than those observed in the corresponding

Table 1 Selected bond distances (Å) and angles (°) for complexes **Sc-1**, **Sc-3**, **Sc-4** and **Y-1**

	Sc{ONNO^{Cum,Me}}(N(SiHMe$_2$)$_2$) (**Sc-1**)	Sc{ONOO^{CumCl}}(N(SiHMe$_2$)$_2$) (**Sc-3**)	Sc{ONOO^{Cum,Cum}}(N(SiHMe$_2$)$_2$) (**Sc-4**)	Y{ONOO^{Cum,Me}}(N(SiHMe$_2$)$_2$)THF (**Y-1**)
M–N(1)	2.341(1)	2.320(2)	2.331(1)	2.611(3)
M–N(2)	2.109(1)	2.095(2)	2.089(1)	2.275(3)
M–N(3)	2.411(1)	—	—	—
M–O(1)	1.968(1)	1.961(2)	1.969(1)	2.151(2)
M–O(2)	1.952(1)	1.947(2)	1.949(1)	2.144(2)
M–O(3)	—	2.268(2)	2.249(1)	2.387(2)
M···Si(1)	3.079	2.937	2.901	3.222
M···Si(2)	3.387	3.433	3.490	3.626
O(1)–M–O(2)	107.34(5)	106.06(7)	104.03(5)	151.76(10)
O(1)–M–O(3)	—	149.12(7)	93.76(5)	90.77(9)
O(2)–M–O(3)	—	92.54(7)	150.18(5)	90.74(9)
N(1)–M–N(2)	154.76(6)	149.07(8)	151.48(5)	152.88(11)
N(1)–M–N(3)	92.14(5)	—	—	—
N(2)–M–N(3)	73.76(5)	—	—	—
Si(1)–N(2)–M	107.16(7)	100.80(10)	99.52(7)	107.95(18)
Si(2)–N(2)–M	124.59(8)	129.11(12)	133.40(8)	129.67(18)
Si(1)–N(2)–Si(2)	126.85(9)	128.62(13)	126.92(9)	122.3(2)

yet six-coordinated yttrium analogues (*vide infra*), reflecting the same difference in ionic radius between scandium and yttrium. The strong difference in the Si(1)–N(2)–Sc and Si(2)–N(2)–Sc bond angles (*ca.* 17–34°; see Table 1) points to monoagostic interactions of one silyl group of the amide ligand with the metal center.[12] Close Sc···Si(1) (2.901–3.079 Å) contacts are accordingly observed, while the other Si(2) atom lies 0.3–0.4 Å further away from the metal center (Table 1).

In **Y-2**, the yttrium atom is six-coordinated by the {ONOO^{Cum,Me}}, amide and THF ligands in a slightly distorted octahedral geometry that is quite similar to that of **Y4**[4a] and related yttrium complexes supported by *tert*-butyl and *p*-CF_3-cumyl-substituted ligands.[3b,4c] One Si–N–Y bond angle is more acute than the other one (107.95(18) *vs.* 129.67(18)°), indicating Si–H···Y monoagostic interaction; similar differences in Si–N–Y bond angles of the Y–N(SiHMe$_2$) moiety have been noted in related 6-coordinate complexes, *e.g.* **Y-4** (111.4(4) *vs.* 135.7(4)°).[4a] On the other hand, as observed previously for **Y4**[4a] and its *p*-CF_3-cumyl-substituted analogue,[3b,4c] the phenyl rings of the two cumyl substituents adopt each an orientation flat parallel to the (THF)O–Y–N(amide) plane. This singular orientation of both cumyl groups can be related to close C–H···π interactions involving hydrogens from THF (contacts: 2.8–3.1 Å) and from Me groups of the N(SiHMe$_2$)$_2$ moiety (contacts: 3.0–3.3 Å) (Fig. 5). Such weak Z–H···π interactions are not seen in the scandium complexes if one excepts a single (possibly incidental) contact between only one phenyl cumyl group and the N(Si*H*Me$_2$)$_2$ hydrogen in **Sc-1** and **Sc-3** (Si–H···π, 3.19 and 2.93 Å, respectively). Note also that the chlorine atoms of the *p*-Cl-cumyl substituents in **Sc-3** are not involved in any peculiar intramolecular interaction.

Ring-opening polymerization of racemic-lactide and *rac*-β-butyrolactone

The prepared {ONXO^{R1,R2}}-scandium- and yttrium-amide complexes were investigated in the stereoselective ROP of *rac*-lactide (*rac*-LA) and *rac*-β-butyrolactone (*rac*-BL) (Scheme 2). In some cases, isopropanol was used as a co-initiator. Representative data from a series of polymerizations conducted in toluene or THF solution are collected in Tables 2 and 3.

All four Sc{ONXO^{R}}(N(SiHMe$_2$)$_2$) complexes promote the controlled ROP of *rac*-LA at 60 °C in toluene (Table 2; entries 2, 4–15), with turnover frequencies (TOF) up to *ca.* 900 mol(LA) mol(Sc)$^{-1}$ h^{-1}. However, they are very poorly active in THF (TOF = *ca.* 1 h^{-1} at 60 °C; entry 2); this observation can likely be accounted for by the competing role of THF *vs. rac*-LA,

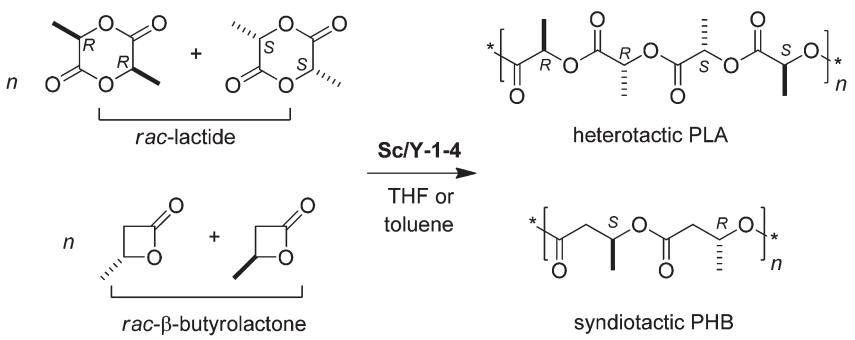

Scheme 2

Table 2 ROP of racemic lactide promoted by {ONXO^{R1,R2}}-scandium and -yttrium catalytic systems[a]

Entry	Complex	$[LA]_0/[M]/[iPrOH]_0$ [a]	Solvent	Temp (°C)	Time[b] (min)	Conv.[c] (%)	$M_{n,theo}$ [d] (g mol^{-1}) (×10^3)	$M_{n,SEC}$ [e] (g mol^{-1}) (×10^3)	$Đ_M$ [e]	P_r [f]
1	**Sc-1**	100 : 1 : 0	THF	20	72 × 60	0	—	—	—	—
2	**Sc-1**	100 : 1 : 0	THF	60	420	5	nd	nd	nd	nd
3	**Sc-1**	100 : 1 : 0	Toluene	20	72 × 60	25	18.0	17.8	1.15	0.82
4	**Sc-1**	100 : 1 : 0	Toluene	60	60	94	13.5	15.4	1.07	0.75
5	**Sc-1**	100 : 1 : 1	Toluene	60	40	99	14.3	14.8	1.11	0.77
6	**Sc-1**	500 : 1 : 1	Toluene	60	180	59	42.5	40.6	1.09	0.77
7	**Sc-2**	100 : 1 : 0	Toluene	60	30	99	14.3	14.6	1.06	0.76
8	**Sc-2**	100 : 1 : 1	Toluene	60	20	99	14.3	15.1	1.08	0.75
9	**Sc-2**	500 : 1 : 1	Toluene	60	120	74	53.3	56.6	1.06	0.77
10	**Sc-3**	100 : 1 : 0	Toluene	60	20	88	12.7	13.2	1.05	0.79
11	**Sc-3**	500 : 1 : 0	Toluene	60	50	50	36.0	32.5	1.06	0.80
12	**Sc-3**	100 : 1 : 1	Toluene	60	15	93	13.4	12.9	1.10	0.80
13	**Sc-4**	100 : 1 : 0	Toluene	60	20	99	14.3	13.9	1.16	0.82
14	**Sc-4**	500 : 1 : 0	Toluene	60	30	85	61.2	66.1	1.07	0.83
15	**Sc-4**	100 : 1 : 1	Toluene	60	10	99	14.3	15.7	1.09	0.83
16	**Y-1**	100 : 1 : 0	Toluene	20	60	99	14.3	17.5	1.97	0.54
17	**Y-1**	100 : 1 : 0	THF	20	20	100	14.4	15.2	1.86	0.73
18	**Y-1**	500 : 1 : 0	THF	20	40	100	72.1	78.5	1.61	0.72
19	**Y-2**	100 : 1 : 0	Toluene	20	60	68	9.8	24.1	1.88	0.50
20	**Y-2**	100 : 1 : 0	THF	20	20	100	14.4	16.7	1.84	0.74
21	**Y-2**	500 : 1 : 0	THF	20	40	100	72.1	80.3	1.70	0.72
22	**Y-3**	100 : 1 : 0	Toluene	20	60	58	8.3	14.5	1.47	0.50
23	**Y-3**	100 : 1 : 0	THF	20	20	99	14.3	17.1	1.55	0.75
24	**Y-3**	500 : 1 : 0	THF	20	40	99	71.3	75.7	1.62	0.74
25	**Y-4**	100 : 1 : 0	THF	20	20	100	14.4	13.0	1.51	0.87
26	**Y-4**	100 : 1 : 1	THF	20	20	100	14.4	12.9	1.12	0.89

[a] All reactions performed with $[rac\text{-LA}]_0$ = 1.0 M. [b] Reaction times were not necessarily optimized. [c] Monomer conversion determined by ^{1}H NMR spectroscopy ($CDCl_3$, 298 K). [d] Theoretical molecular weight calculated using $M_{n,\,theo}$ = conv(LA) × $[rac\text{-LA}]_0/[M \text{ or } iPrOH]$ × M_{LA}. [e] Experimental molecular weight determined by SEC *vs.* polystyrene standards and corrected by a factor of 0.58; $Đ_M = M_w/M_n$. [f] P_r is the probability of racemic linkage between monomer units, as determined from the methine region of the homonuclear decoupled ^{1}H NMR spectrum.

Table 3 ROP of racemic β-butyrolactone promoted by {ONXO^{R1,R2}}-yttrium catalytic systems[a]

Entry	Complex	$[BL]_0/[M]/[iPrOH]_0$ [a]	Temp (°C)	Time[b] (min)	Conv.[c] (%)	$M_{n,theo}$ [d] (g mol^{-1}) (×10^3)	$M_{n,SEC}$ [e] (g mol^{-1}) (×10^3)	$Đ_M$ [e]	P_r [f]	B[g]
27	**Y-1**	100 : 1 : 0	20	2	98	8.4	31.6	1.39	0.81	1.2
28	**Y-1**	500 : 1 : 0	20	10	90	38.7	157.5	1.45	0.84	1.3
29	**Y-1**	100 : 1 : 1	20	0.5	100	8.6	26.2	1.08	0.85	1.3
30	**Y-1**	100 : 1 : 1	20	0.33	87	7.5	22.1	1.06	0.85	1.3
31	**Y-2**	100 : 1 : 0	20	1	92	7.9	33.3	1.63	0.82	1.6
32	**Y-2**	500 : 1 : 0	20	5	86	37.0	183.5	1.87	0.85	1.7
33	**Y-2**	100 : 1 : 1	20	0.5	85	7.3	31.2	1.74	0.85	1.7
34	**Y-3**	100 : 1 : 0	20	1	100	8.6	31.3	1.83	0.86	1.6
35	**Y-3**	500 : 1 : 0	20	5	100	43.0	121.9	1.41	0.87	1.6
36	**Y-3**	100 : 1 : 1	20	0.5	78	6.7	26.3	1.32	0.87	1.6
37	**Y-4**	100 : 1 : 0	20	1	95	8.2	34.3	1.16	0.88	1.3

[a] All reactions performed with $[rac\text{-BL}]_0$ = 2.4 M in toluene. [b] Reaction times were not necessarily optimized. [c] BL conversion to PHB determined by ^{1}H NMR spectroscopy ($CDCl_3$, 298 K) on the crude reaction mixture. [d] Theoretical molecular weight calculated using $M_{n,\,theo}$ = conv(BL) × $[rac\text{-BL}]_0/[Y \text{ or } iPrOH]$ × M_{BL}. [e] Experimental (uncorrected) molecular weight determined by SEC in $CHCl_3$; $Đ_M = M_w/M_n$. [f] P_r is the probability of racemic linkage between monomer units and is determined by $^{13}C\{^1H\}$ NMR spectroscopy. [g] Bernoulli model triad test *B*, where $B = (ii)(ss)/[(is) + (si)]^2$.

preventing coordination of the later monomer onto the active metal site. In fact, these scandium catalysts are systematically less active than their yttrium analogues, which operate at room temperature, in toluene and even faster so in THF (entries 16–26; compare entries 16/17, 19/20, 22/23), with TOF up to *ca.* 750 mol(LA) mol(Y) $^{-1}$ h^{-1}; scandium complexes **Sc-1–Sc-4** are very poorly active at 20 °C in toluene and essentially inactive in THF at this temperature (see *e.g.* entries 1 and 3). Slower reactivity of scandium *vs.* yttrium and lutetium systems was previously noted in several instances in the literature.[6a,i,j,13] No dramatic change in activity was observed within the series **Sc-1–Sc-4**, although the Me_2N-capped complex (**Sc-1**) appeared somewhat less active than the OMe-capped systems (compare *e.g.* entry 6, TOF = 100 h^{-1} *vs.* entry 9, TOF = 185 h^{-1}); the reverse trend is observed with yttrium complexes (compare entries 16 *vs.* 19 and 22).

On the other hand, the degree of control of the scandium catalyst systems over the molecular weights is remarkable,

with experimental M_n values (determined by SEC) in excellent agreement with the calculated ones and quite narrow dispersities ($Đ_M$ < 1.1 in nearly all cases; entries 3–15). This latter parameter control compares favorably with that of yttrium-amide analogues, which provide much broader (yet still unimodal) molecular weight distributions ($Đ_M$ = 1.5–2.0).[14] It is thus noteworthy that the scandium-amide complexes themselves are excellent initiators, since they offer the same control over the molecular weights (*i.e.*, 100% initiation efficiency and narrow dispersities) as the corresponding isopropoxide complexes generated *in situ* with 1 equiv. of isopropanol. This is in contrast to yttrium catalysts, for which only addition of 1 (or more) equiv. of isopropanol onto the amide precursors allowed achieving truly narrow molecular weight distributions (*e.g.*, compare entries 25 and 26 in Table 2, and refer to earlier reports[3b]). In addition, the PLAs produced with these Sc complexes did not exhibit significant transesterification side-processes, as a single population of macromolecules with 144 Da increments was observed by MALDI-ToF mass spectrometry (see Fig. S38 in the ESI†); this also allowed us to identify unambiguously the expected $-OCH(CH_3)_2$ and –OH termini when isopropanol was used as a co-initiator.

The ROP of *rac*-LA promoted by scandium complexes **Sc-1–Sc-4** in toluene allowed the formation of highly heterotactic-enriched PLAs, with the probability of racemic linkages between monomer units (P_r) in the range 0.75–0.83 (Table 2, entries 3–15). As anticipated for a regular coordination–insertion mechanism, for a given ligand system, these stereoselectivity values are not affected by the nature of the initiating group (amide or *in situ*-generated isopropoxide), consistent with positioning of this group at the terminus of the propagating chain (this also stands for yttrium complexes, compare entries 25 and 26). Although noticeable, only a marginal variation of the stereoselectivity was observed within the **Sc-1–Sc-4** series: the *o*,*p*-dicumyl-substituted catalyst **Sc-4** is just slightly more stereoselective than the other ones. This contrasts with the neat increase in heterotacticity between **Y-4** (P_r = 0.87–0.89) and the other three yttrium catalysts (P_r = 0.72–0.75). We assume that this difference in stereocontrol between **Sc-4** and **Y-4**, as compared to their *p*-methyl-substituted **Sc/Y-1–Sc/Y-3** analogues, reflects the similar highly sterically crowded environment in the four scandium systems, while with the larger yttrium center,[7] the *o*,*p*-dicumyl-substituted ligand enables us to make a further increase in steric hindrance. Interestingly yet, the scandium systems **Sc-1–Sc-3** are systematically more stereoselective than their yttrium analogues, not only in toluene where they are essentially atactic (P_r = 0.50–054) but also in THF (P_r = 0.72–0.75). In contrast to earlier observations on the *p*-CF_3-substituted cumyl system,[4c] the *p*-Cl-substituted cumyl ligand (**L3**), ever associated with scandium or yttrium (**Sc**/**Y-3**), does not show decreased stereoselectivity as compared to the regular (non-substituted) cumyl systems (**Sc**/**Y-2**); this is likely accounted for by the significantly lower electron-withdrawing ability of Cl as compared to CF_3.

In line with the moderate activity noted above in the ROP of *rac*-LA, none of the scandium complexes **Sc-1–Sc-4** proved active for the ROP of *rac*-BL under the conditions investigated (toluene, 60 °C, 24 h; $[BL]_0$–$[Sc]$–$[iPrOH]_0$ = 100 : 1 : 0 or 100 : 1 : 1). It is indeed well-known that this monomer is much more reluctant to ring-open and its polymerization requires highly active catalysts.[1d,f,4] In fact, yttrium complexes **Y-1–Y-4** showed interesting performance in the ROP of *rac*-BBL in toluene solution at 20 °C (Table 3, entries 27–37).[15] As earlier noted for yttrium complexes of this class,[4] all the PHBs formed under those conditions had unimodal, although broadened molecular distributions ($Đ_M$ = 1.08–1.87); the SEC (uncorrected) molecular weights, in the range 22.1–183.5 × 10^3 g mol^{-1}, follow monotonously the theoretical values calculated from the monomer-to-metal center or the added alcohol ratio. ^{13}C NMR analysis revealed that all those PHBs had a significantly syndiotactic-enriched microstructure, with P_r in the range 0.81–0.88. The Bernoulli triad model test *B* was in all cases close to 1, consistent with a chain-end stereocontrol mechanism.[1d,f,4] As noted for *rac*-LA polymerizations, only a marginal variation of the stereoselectivity was observed within the **Y-1–Y-4** series.

Conclusions

Due to its quite small ionic radius, scandium forms 5-coordinate amide complexes with the tetradentate, dianionic $\{ONXO^{R1,R2}\}^{2-}$ ligands incorporating bulky *ortho*-cumyl R^1 substituents. This contrasts with previous reports on 6-coordinate scandium chloro complexes incorporating related tetradentate diamino-bis(phenolate) ligands with *ortho*-*t*Bu R^1 substituents.[8] This contrasts also with the analogous, but 6-coordinate yttrium complexes $Y\{ONXO^{Cum,R2}\}(N(SiHMe_2)_2)(THF)$, which all incorporate a coordinated THF molecule. $Sc\{ONXO^{Cum,R2}\}(N(SiHMe_2)_2)$ complexes are less active than their yttrium analogues for promoting the ROP of racemic lactide and are inactive in the ROP of the more demanding racemic β-butyrolactone. On the other hand, these scandium amide complexes feature a significantly improved control of the ROP of lactide, with much narrower molecular weight distributions and higher heteroselectivities. These reactivity and selectivity trends can be rationalized by a much more sterically crowded coordination sphere in scandium than in yttrium complexes.

Experimental section

General considerations

All manipulations were performed under a purified argon atmosphere using standard Schlenk techniques or in a glovebox (<1 ppm O_2, <5 ppm H_2O). Solvents were distilled from Na/benzophenone (THF and Et_2O) or Na/K alloy (toluene, hexane and pentane) under argon, degassed thoroughly and stored under argon prior to use. Benzene-d_6 and toluene-d_8 (>99.5% D, Eurisotop) used for NMR of complexes were stored over Na/K alloy and vacuum-transferred just before use. Pro-ligand **L4** was prepared following the literature procedure.[3b,4c] Starting

materials for the synthesis of pro-ligands **L1**, **L2** and **L3** were purchased and used without further purification. Rare earth precursors $Ln[N(SiHMe_2)_2]_3(THF)$ (Ln = Y, Sc) were synthesized by literature procedures.[16] Racemic lactide (*rac*-LA) was obtained from Aldrich and racemic β-butyrolactone (*rac*-BL) from TCI. Purification of *rac*-LA required a three-step procedure involving first a recrystallization from a hot, concentrated iPrOH solution (80 °C), followed by two subsequent recrystallizations in hot toluene (100 °C). Racemic β-butyrolactone was freshly distilled from CaH_2 under argon prior to use. After purification, *rac*-LA and *rac*-BL were stored at a temperature of −30 °C in the glovebox.

Instrumentation and measurements

NMR spectra of complexes were recorded on Bruker AC-300, Avance DRX 400 and AM-500 spectrometers in Teflon-valved NMR tubes at 25 °C unless otherwise indicated. ^1H and ^{13}C NMR chemical shifts are reported in ppm *vs*. $SiMe_4$ and were determined by reference to the residual solvent peaks. Assignment of resonances for organometallic complexes was made from 2D ^1H–^{13}C HMQC and HMBC NMR experiments. ^{29}Si chemical shifts were determined by external reference to $SiMe_4$.

Elemental analyses (C, H, N) were performed using a Flash EA1112 CHNS Thermo Electron apparatus and results shown are the average of two independent measurements.

Size exclusion chromatography (SEC) analyses of PLAs were performed in THF (1.0 mL min^{-1}) at 20 °C using a Polymer Laboratories PL-GPC 50 plus apparatus equipped with two ResiPore 300 × 7.5 mm columns, and RI and Dual angle LS (PL-LS 45/90) detectors. The number-average molecular masses (M_n) and dispersity ($Đ_M = M_w/M_n$) of the polymers were calculated with reference to a universal calibration *vs*. polystyrene standards. Reported experimental SEC molar mass values ($M_{n,SEC}$) for PLA samples were corrected by a factor of 0.58 as previously established.[17] $M_{n,SEC}$ values for PHB samples are uncorrected. Unless otherwise stated, the SEC traces of the polymers all exhibited a unimodal, and usually symmetrical, peak.

MALDI-ToF mass spectra were obtained with a Bruker Daltonic MicroFlex LT, using a nitrogen laser source (337 nm, 3 ns) in linear mode with a positive acceleration voltage of 20 kV and using α-cyano-4-hydroxycinnamic acid as the matrix.

$\{ONNO^{Cum,Me}\}H_2$ (L1). *N*,*N*-Dimethylethylenediamine (1.35 mL, 1.09 g, 12.35 mmol) and aqueous paraformaldehyde (1.85 mL of a 37 wt% solution in water, 24.7 mmol) were added to a solution of 4-methyl-2-(2-phenylpropan-2-yl)phenol (5.60 g, 24.7 mmol) in methanol (25 mL). The reaction mixture was heated under stirring for 72 h at 80 °C. Upon cooling, a white precipitate formed, which was isolated by filtration, washed with ice-cold methanol (3 × 20 mL) and dried *in vacuo* to yield a fine white powder (2.90 g, 41%). ^1H NMR (500 MHz, $CDCl_3$, 298 K): δ 1.47 (s, 6H, ArCH_3), 1.71 (t, ^3J = 5.0 Hz, 2H, NCH_2CH_2N), 1.79 (s, 12H, $C(CH_3)CH_3$), 1.99 (t, ^3J = 5.0 Hz, 2H, NCH_2CH_2N), 2.28 (s, 6H, $N(CH_3)_2$), 3.18 (s, 2H, NCH_2Ar), 7.36–6.65 (m, 14H, Haro), 9.36 (s, 2H, O*H*). $^{13}C\{^1H\}$ NMR ($CDCl_3$, 125 MHz, 298 K): δ 21.2 (Ar*C*H_3), 29.7 ($C(CH_3)_2$), 42.2 ($C(CH_3)_2$), 44.5 ($NCH_2CH_2NMe_2$), 49.1 ($NCH_2CH_2NMe_2$), 56.2 ($NCH_2CH_2NMe_2$), 56.6 ($ArCH_2N$), 122.9, 124.8, 126.3, 126.6, 127.6, 127.7, 129.4, 136.8 (aryl-*C*H), 151.8, 153.2 (aryl-*C*). Elem. Anal. Calcd for $C_{38}H_{48}N_2O_2$: C, 80.81; H, 8.57; N, 4.96; found: C, 80.96; H, 8.82; N, 4.93.

$\{ONOO^{Cum,Me}\}H_2$ (L2). This compound was prepared in an analogous manner to that described above for **L1**, starting from 2-methoxyethylamine (1.35 mL, 1.16 g, 15.5 mmol), aqueous paraformaldehyde (2.32 mL of a 37 wt% solution in water, 30.9 mmol) and 4-methyl-2-(2-phenylpropan-2-yl) phenol[18] (7.00 g, 30.9 mmol). Workup afforded **L2** as a fine white powder (3.10 g, 36%). ^1H NMR (500 MHz, toluene-d_8, 298 K): δ 1.71 (s, 12H, $C(CH_3)CH_3$), 2.31 (s, 6H, ArCH_3), 2.48 (t, ^3J = 5.0 Hz, 2H, OCH_2CH_2N), 2.99 (s, 3H, OCH_3), 3.08 (t, ^3J = 5.0 Hz, 2H, OCH_2CH_2N), 3.59 (s, 2H, NCH_2Ar), 7.29–6.74 (m, 14H, Haro), 7.71 (s, 2H, O*H*). $^{13}C\{^1H\}$ NMR ($CDCl_3$, 125 MHz, 298 K): δ 21.2 (Ar*C*H_3), 29.8 ($C(CH_3)_2$), 42.2 ($C(CH_3)_2$), 51.4 (NCH_2CH_2OMe), 56.8 ($ArCH_2N$), 58.8 (OCH_3), 71.2 (NCH_2CH_2OMe), 123.5, 125.5, 126.2, 127.4, 127.7, 128.2, 129.5, 136.4 (aryl-*C*H), 151.0, 152.6 (aryl-*C*). Elem. Anal. Calcd for $C_{37}H_{45}NO_3$: C, 80.54; H, 8.22; N, 2.54; found: C, 80.63; H, 8.29; N, 2.51.

$\{ONOO^{CumCl,Me}\}H_2$ (L3). (A) 4-Methyl-2-(2-(4-chlorophenyl) propan-2-yl)phenol: A Schlenk flask was charged with $AlCl_3$ (0.090 g, 0.655 mmol) and *p*-cresol (0.710 g, 6.55 mmol), and then heated for 30 min at 160 °C until a melt of aluminum phenolate is formed. The mixture was cooled down to 60 °C. 2-(4-Chlorophenyl)propene (0.200 g, 1.31 mmol) was added, and the reaction was stirred for 18 h at 30 °C. The reaction mixture was cooled down to room temperature and diluted with water (*ca*. 10 mL) and $CHCl_3$ (*ca*. 15 mL). The organic layer was separated and treated with 5% aqueous H_2SO_4 (5 mL) and then 5% aqueous KOH (5 mL). The combined organic extracts were dried over anhydrous sodium sulfate and then concentrated under vacuum. The crude material was purified by chromatography through a plug of silica gel using CH_2Cl_2–petroleum ether (1 : 1) as the eluent. 4-Methyl-2-(2-(4-chlorophenyl)propan-2-yl)phenol was isolated as a pale yellow oil (1.36 g, 80%). ^1H NMR (400 MHz, $CDCl_3$, 298 K): δ 1.56 (s, 6H, $C(CH_3)_2$), 2.25 (s, 3H, CH_3), 4.33 (s, 1H, O*H*), 6.52 (d, J = 8.0 Hz, 1H, H_{aro} *o*-OH), 6.87 (d, J = 8.0 Hz, 1H, H_{aro} *m*-OH), 7.28–7.04 (m, 5H, H_{ArOCl} and H_{Ar} *meta* OH). $^{13}C\{^1H\}$ NMR (100 MHz, $CDCl_3$, 298 K): δ 21.0 (Ar*C*H_3), 29.6 ($C(CH_3)_2$), 41.4 ($C(CH_3)_2$, 117.5, 127.2, 127.5, 128.6, 129.0, 129.8 (aryl-*C*H), 147.7 (aryl-*C*), 151.4 (C_{ArOH}).

(B) Pro-ligand L3: This was prepared in an analogous manner to that described above for **L1**, starting from 2-methoxyethylamine (0.103 g, 1.35 mmol), aqueous paraformaldehyde (0.235 g of a 37 wt% solution, 2.85 mmol) and 4-methyl-2-(2-(4-chlorophenyl)propan-2-yl)phenol (0.750 g, 2.85 mmol) in methanol (2 mL). The reaction was stirred for 24 h at 90 °C. Workup afforded crude **L3** as a white powder, which was recrystallized from isopropanol at −30 °C to give colorless crystals of analytically pure **L3** (0.80 g, 90%); some of these crystals proved suitable for X-ray diffraction studies. M.p. = 125 °C.

^{1}H NMR (400 MHz, $CDCl_3$, 298 K): δ 1.56 (s, 12H, C(CH_3)$_2$), 2.20 (s, 6H, ArCH_3), 2.36 (t, J = 5.3 Hz, 2H, NCH_2CH$_2$OMe), 2.87 (overlapped s and t, 5H, OCH_3 and NCH$_2$CH_2OMe), 3.47 (s, 4H, ArCH_2N), 6.64 (br s, 2H, m-H_{ArOH}), 7.12–7.06 (m, 10H, H_{Ar}), 7.79 (br s, 2H, OH). ^{13}C{^{1}H} NMR (100 MHz, $CDCl_3$, 298 K): δ 20.9 (ArCH$_3$), 29.5 (C(CH$_3$)$_2$), 41.5 (C(CH$_3$)$_2$), 51.2 (NCH$_2$CH$_2$OMe), 57.2 (ArCH$_2$N), 58.4 (OCH$_3$), 71.3 (NCH$_2$$CH_2$OMe), 122.9, 127.1, 127.3, 127.5, 127.6, 129.3, 130.4, 138.8 (aryl-CH), 149.9 (aryl-C), 152.2 (C_{ArOH}). ESI-HRMS: m/z calcd for $C_{37}H_{44}NO_3Cl_2$ (M + H)$^+$: 620.2698; found: 620.2692. Anal. Calcd for $C_{37}H_{43}NO_3Cl_2$: C, 71.60; H, 6.98; N, 2.26; found: C, 71.52; H, 7.06; N, 2.23.

Sc{ONNO^{Cum,Me}}(N(SiHMe$_2$)$_2$) (Sc-1). A Schlenk flask was charged with {ONNO^{Cum,Me}}H$_2$ (1.00 g, 1.77 mmol) and Sc[N(SiHMe$_2$)$_2$]$_3$(THF) (0.910 g, 1.77 mmol), and toluene (*ca.* 10 mL) was vacuum transferred at room temperature. The reaction mixture was stirred overnight at 50 °C. Volatiles were then removed under vacuum, and the residue was washed with hexane (2 × 3 mL) and dried under vacuum to give **Sc-1** as a white powder (0.96 g, 73%). Dissolution of this solid in heptane and recrystallization at room temperature for 15 days afforded **Sc-1** as analytically pure colorless crystals, some of which proved suitable for X-ray diffraction studies. ^{1}H NMR (400 MHz, C_6D_6, 338 K): δ 0.34 (d, $^3J_{H-H}$ = 2.6 Hz, 12H, SiH(CH_3)$_2$), 1.58 (m, 2H, NCH_2CH$_2$N(CH$_3$)$_2$), 1.64 (s, 6H, NCH$_2$CH$_2$N(CH_3)$_2$), 1.87 (s, 6H, C(CH_3)$_2$), 1.91 (s, 6H, C(CH_3)$_2$), 2.06–2.08 (m, 2H, NCH$_2$CH_2N(CH$_3$)$_2$), 2.26 (s, 6H, ArCH_3), 3.24 (br, 4H, ArCH_2), 5.03 (sept, $^3J_{H-H}$ = 2.6 Hz, 2H, SiH(CH$_3$)$_2$), 6.59 (s, 2H, Haro), 6.95–6.99 (m, 2H, Haro), 7.11 (t, J_{H-H} = 7.6 Hz, 4H, Haro), 7.20 (s, 2H, Haro), 7.34–7.36 (m, 4H, Haro). ^{13}C{^{1}H} NMR (100 MHz, C_6D_6, 338 K): δ 3.26 (SiH(CH$_3$)$_2$), 20.5 (ArCH$_3$), 26.3 (C(CH$_3$)$_2$), 29.4 (C(CH$_3$)$_2$), 31.3 (C(CH$_3$)$_2$), 35.3 (C(CH$_3$)$_2$), 42.4 (C(CH$_3$)$_2$), 46.9 (NCH$_2$CH$_2$N(CH$_3$)$_2$), 52.9 (NCH$_2$$CH_2$N(CH$_3$)$_2$), 58.4 (N$CH_2CH_2$N(CH$_3$)$_2$), 61.6 (Ar$CH_2$), 124.2 (aryl-$C$q), 124.5 (aryl-$C$q), 124.8 (aryl-$C$H), 126.2 (aryl-$C$H), 127.4 (aryl-$C$H), 127.6 (aryl-$C$H), 128.8 (aryl-$C$H), 129.2 (aryl-$C$H), 135.9 (aryl-$C$q), 151.6 (aryl-$C$q), 159.5 (aryl-$C$q). ^{29}Si{^{1}H} NMR (79 MHz, C_6D_6, 338 K): δ −20.85 (s). ^{29}Si NMR (79 MHz, C_6D_6, 338 K): δ −20.85 (doublet of multiplets, $^1J_{Si-H}$ = 170 Hz, $^2J_{Si-H}$ = 7.1 Hz). Anal. Calcd for $C_{42}H_{60}N_3O_2ScSi_2$: C, 68.16; H, 8.17; N, 5.68; found: C, 68.01; H, 8.18; N, 5.74.

Sc{ONOO^{Cum,Me}}(N(SiHMe$_2$)$_2$) (Sc-2). This product was prepared as described above for **Sc-1** starting from {ONOO^{Cum,Me}}H$_2$ (1.00 g, 1.81 mmol) and Sc[N(SiHMe$_2$)$_2$]$_3$(THF) (0.930 g, 1.81 mmol) to give **Sc-2** as a white powder (0.84 g, 64%). ^{1}H NMR (500 MHz, C_6D_6, 298 K): δ 0.34 (d, $^3J_{H-H}$ = 2.7 Hz, 12H, SiH(CH_3)$_2$), 1.86 (s, 6H, C(CH_3)$_2$), 1.91 (s, 6H, C(CH_3)$_2$), 1.94 (d, $^3J_{H-H}$ = 5.7 Hz, 2H, NCH_2CH$_2$OCH$_3$), 2.11 (br, 2H, ArCH_2), 2.28 (s, 6H, ArCH_3), 2.38 (br, 2H, ArCH_2), 2.56 (d, $^3J_{H-H}$ = 5.5 Hz, 2H, NCH$_2$CH_2OCH$_3$), 2.79 (s, 3H, NCH$_2$CH$_2$OCH_3), 4.90 (hept, $^3J_{H-H}$ = 2.7 Hz, 2H, HSi(CH$_3$)$_2$), 6.56 (s, 2H, Haro), 7.02–7.06 (m, 2H, Haro), 7.16–7.20 (m, 4H, Haro), 7.23 (d, J_{H-H} = 1.7 Hz, 2H, Haro), 7.40 (d, J_{H-H} = 7.5 Hz, 4H, Haro). ^{13}C{^{1}H} NMR (125 MHz, C_6D_6, 298 K): δ 2.75 (SiH(CH$_3$)$_2$), 20.7 (ArCH$_3$), 29.6 (C(CH$_3$)$_2$), 30.4 (C(CH$_3$)$_2$), 42.4 (C(CH$_3$)$_2$), 55.1 (NCH$_2$CH$_2$OCH$_3$), 61.3 (ArCH$_2$), 61.8 (NCH$_2$CH$_2$OCH$_3$), 71.6 (NCH$_2$$CH_2OCH_3$), 124.1 (aryl-$C$q), 124.8 (aryl-$C$H), 126.2 (aryl-$C$H), 127.6 (aryl-$C$q), 127.7 (aryl-$C$H), 128.7 (aryl-$C$H), 128.9 (aryl-$C$H), 136.2 (aryl-$C$q), 151.4 (aryl-$C$q), 159.5 (aryl-$C$q). Anal. Calcd for $C_{41}H_{57}N_2O_3ScSi_2$: C, 67.73; H, 7.90; N, 3.85; found: C, 67.60; H, 7.96; N, 3.79.

Sc{ONOO^{CumCl,Me}}(N(SiHMe$_2$)$_2$) (Sc-3). This product was prepared as described above for **Sc-1**, starting from {ONOO-^{CumCl,Me}}H$_2$ (0.100 g, 0.161 mmol) and Sc[N(SiHMe$_2$)$_2$]$_3$(THF) (0.083 g, 0.161 mmol) to give **Sc-3** as a white powder (0.090 g, 70%). ^{1}H NMR (400 MHz, C_6D_6, 298 K): δ 0.27 (d, $^3J_{H-H}$ = 3.0 Hz, 12H, SiH(CH_3)$_2$), 1.72 (s, 6H, C(CH_3)$_2$), 1.80 (s, 6H, C(CH_3)$_2$), 1.97 (t, $^3J_{H-H}$ = 5.7 Hz, 2H, NCH_2CH$_2$OCH$_3$), 2.27 (s, 6H, ArCH_3), 2.37 (br, 2H, ArCH_2), 2.58 (t, $^3J_{H-H}$ = 5.7 Hz, 2H, NCH_2CH$_2$OCH$_3$), 2.90 (s, 3H, NCH$_2$CH$_2$OCH_3), 3.13–3.16 (m, 2H, ArCH_2), 4.78 (hept, $^3J_{H-H}$ = 3.0 Hz, 2H, SiH(CH$_3$)$_2$), 6.55 (d, J_{H-H} = 1.4 Hz, 2H, Haro), 6.99–7.02 (m, 1H, Haro), 7.10–7.12 (m, 1H, Haro), 7.16–7.18 (m, 2H, Haro). ^{13}C{^{1}H} NMR (100 MHz, C_6D_6, 298 K): δ 2.5 (SiH(CH$_3$)$_2$), 20.6 (ArCH$_3$), 29.4 (C(CH$_3$)$_2$), 30.3 (C(CH$_3$)$_2$), 41.9 (C(CH$_3$)$_2$), 55.5 (NCH$_2$CH$_2$OCH$_3$), 61.4 (ArCH$_2$), 61.8 (NCH$_2$CH$_2$OCH$_3$), 71.7 (NCH$_2$$CH_2OCH_3$), 124.3 (aryl-$C$q), 124.4 (aryl-$C$q), 127.7 (aryl-$C$H), 127.8 (aryl-$C$H), 128.2 (aryl-$C$H), 128.6 (aryl-$C$H), 128.8 (aryl-$C$H), 128.9 (aryl-$C$H), 130.5 (aryl-$C$q), 135.7 (aryl-$C$q), 150.2 (aryl-$C$q), 159.3 (aryl-$C$q). ^{29}Si{^{1}H} NMR (79 MHz, C_6D_6, 298 K): δ −19.79 (s). ^{29}Si NMR (79 MHz, C_6D_6, 298 K): δ −19.79 (d of multiplets, $^1J_{Si-H}$ = 162 Hz, $^2J_{Si-H}$ = 6.6 Hz). Anal. Calcd for $C_{41}H_{55}Cl_2N_2O_3ScSi_2$: C, 61.87; H, 6.97; N, 3.52; found: C, 61.75; H, 7.02; N, 3.58.

Sc{ONOO^{Cum,Cum}}(N(SiHMe$_2$)$_2$) (Sc-4). This product was prepared as described above for **Sc-1** starting from {ONOO^{Cum,Cum}}H$_2$ (0.200 g, 0.263 mmol) and Sc[N(SiHMe$_2$)$_2$]$_3$(THF) (0.135 g, 0.263 mmol) to give **Sc-4** as a white powder (0.160 g, 65%). ^{1}H NMR (400 MHz, C_6D_6, 333 K): δ 0.29 (d, $^3J_{H-H}$ = 3.0 Hz, 6H, SiH(CH_3)$_2$), 0.33 (br d, 6H, SiH(CH_3)$_2$), 1.57 (s, 6H, C(CH_3)$_2$), 1.63–1.65 (m, 12H, C(CH_3)$_2$), 1.88 (d, $^3J_{H-H}$ = 3.4 Hz, 2H, C(CH_3)$_2$), 2.02–2.06 (m, 3H, ArCH_2 + NCHHCH$_2$OCH$_3$), 2.57 (s, 1H, NCHHCH$_2$OCH$_3$), 2.69 (t, $^3J_{H-H}$ = 5.7 Hz, 2H, NCH$_2$CH_2OCH$_3$), 2.93 (s, 2H, NCH$_2$CH$_2$OCH_3), 3.10–3.20 (s, 3H, ArCH_2), 4.86 (hept, $^3J_{H-H}$ = 3.0 Hz, 1H, SiH(CH$_3$)$_2$), 5.01 (br, 1H, SiH(CH$_3$)$_2$), 6.67 (d, J_{H-H} = 2.4 Hz, 1H, Haro), 6.99–7.13 (m, 11H, Haro), 7.17–7.20 (m, 4H, Haro), 7.26–7.28 (m, 5H, Haro), 7.35–7.37 (m, 3H, Haro). ^{13}C{^{1}H} NMR (100 MHz, C_6D_6, 333 K): δ 2.6 (SiH(CH$_3$)$_2$), 3.2 (SiH(CH$_3$)$_2$), 29.5 (C(CH$_3$)$_2$), 30.1 (C(CH$_3$)$_2$), 30.2 (ArCH$_2$), 30.7 (C(CH$_3$)$_2$), 30.8 (C(CH$_3$)$_2$), 30.9 (C(CH$_3$)$_2$), 31.0 (C(CH$_3$)$_2$), 42.1 (C(CH$_3$)$_2$), 42.2 (C(CH$_3$)$_2$), 42.3 (C(CH$_3$)$_2$), 42.6 (C(CH$_3$)$_2$), 42.8 (C(CH$_3$)$_2$), 43.5 (C(CH$_3$)$_2$), 55.3 (NCH$_2$CH$_2$OCH$_3$), 61.4 (ArCH$_2$), 61.9 (NCH$_2$CH$_2$OCH$_3$), 71.7 (NCH$_2$$CH_2OCH_3$), 123.8 (aryl-$C$q), 124.8 (aryl-$C$H), 125.1 (aryl-$C$H), 125.2 (aryl-$C$H), 125.3 (aryl-$C$H), 125.5 (aryl-$C$H), 125.9 (aryl-$C$H), 126.2 (aryl-$C$H), 126.5 (aryl-$C$H), 126.6 (aryl-$C$H), 126.7 (aryl-$C$H), 126.8 (aryl-$C$H), 127.1 (aryl-$C$H), 127.6 (aryl-$C$H), 127.7 (aryl-$C$H), 127.8 (aryl-$C$H), 127.9 (aryl-$C$H), 128.1 (aryl-$C$H), 128.8 (aryl-$C$H), 129.0 (aryl-$C$H), 135.2 (aryl-$C$q), 135.6 (aryl-$C$q), 135.7 (aryl-$C$q), 136.1 (aryl-$C$q), 137.4 (aryl-$C$q), 137.7 (aryl-$C$q), 137.8 (aryl-$C$q), 138.8 (aryl-$C$q), 151.2 (aryl-$C$q), 151.4 (aryl-$C$q), 151.6 (aryl-$C$q), 151.7 (aryl-$C$q), 151.9 (aryl-$C$q),

153.1 (aryl-*C*q), 158.9 (aryl-*C*q), 159.5 (aryl-*C*q), 159.7 (aryl-*C*q), 160.2 (aryl-*C*q). ^{29}Si{^{1}H} NMR (79 MHz, C_6D_6, 333 K): δ −20.40 (br s), −20.30 (s). ^{29}Si NMR (79 MHz, C_6D_6, 333 K): δ −20.31 (d of multiplets, $^1J_{Si-H}$ = 171.6 Hz, $^2J_{Si-H}$ = 6.5 Hz). Anal. Calcd for $C_{57}H_{73}N_2O_3ScSi_2$: C, 73.19; H, 7.87; N, 3.00; found: C, 73.24; H, 7.96; N, 3.09.

NMR-scale generation of Y{ONNO^{Cum,Me}}(N(SiHMe$_2$)$_2$) (Y-1). A J. Young NMR-tube was charged with {ONNO^{Cum,Me}}H_2 (0.050 g, 0.088 mmol) and Y[N(SiHMe$_2$)$_2$]$_3$(THF) (0.049 g, 0.088 mmol), and benzene-d_6 (*ca*. 0.6 mL) was added at room temperature. NMR monitoring revealed rapid, quantitative conversion of the reagents to the targeted complex, with release of two equiv. of HN(SiHMe$_2$)$_2$. ^{1}H NMR (400 MHz, C_6D_6, 313 K): δ 0.42 (d, $^3J_{H-H}$ = 2.8 Hz, 12H, SiH(CH_3)$_2$), 1.29 (m, 4H, α-CH_2 THF), 1.64 (br s, 2H, ArCH_2), 1.71 (s, 6H, NCH$_2$CH$_2$N(CH_3)$_2$), 1.85 (s, 6H, C(CH_3)$_2$), 2.06 (s, 6H, C(CH_3)$_2$), 2.31 (s, 8H, ArCH_2 + ArCH_3), 2.77 (d, $^3J_{H-H}$ = 12.5 Hz, 2H, NCH$_2$CH_2N(CH$_3$)$_2$), 3.31 (br s, 4H, β-CH_2 THF), 3.64 (d, $^3J_{H-H}$ = 12.5 Hz, 2H, NCH_2CH$_2$N(CH$_3$)$_2$), 4.80–4.82 (m, 2H, *H*Si(CH$_3$)$_2$), 6.78 (d, J_{H-H} = 1.6 Hz, 2H, Haro), 6.95 (d, J_{H-H} = 7.3 Hz, 2H, Haro), 7.10–7.14 (m, 4H, Haro), 7.26 (d, J_{H-H} = 1.7 Hz, 2H, Haro), 7.39 (d, J_{H-H} = 7.3 Hz, 4H, Haro). ^{13}C NMR (100 MHz, C_6D_6, 313 K): δ 4.4 (SiH(*C*H$_3$)$_2$), 20.6 (ArCH_3), 24.8 (α-*C*H$_2$ THF), 29.1 (C(*C*H$_3$)$_2$), 31.6 (C(*C*H$_3$)$_2$), 42.4 (*C*(CH$_3$)$_2$), 45.3 (NCH$_2$CH$_2$N(*C*H$_3$)$_2$), 48.7 (N*C*H$_2$CH$_2$N(CH$_3$)$_2$), 60.0 (Ar*C*H$_2$), 64.9 (N*C*H$_2$CH$_2$N(CH$_3$)$_2$), 66.9 (β-*C*H$_2$ THF), 122.3 (aryl-*C*q), 124.3 (aryl-*C*H), 124.9 (aryl-*C*q), 126.4 (aryl-*C*H), 127.5 (aryl-*C*H), 129.3 (aryl-*C*H), 129.8 (aryl-*C*H), 136.3 (aryl-*C*q), 152.6 (aryl-*C*q), 161.4 (aryl-*C*q).

NMR-scale generation of Y{ONOO^{Cum,Me}}(N(SiHMe$_2$)$_2$) (Y-2). This product was prepared *in situ* as described above for **Y-1**, starting from {ONOO^{Cum,Me}}H_2 (0.050 g, 0.091 mmol) and Y[N(SiHMe$_2$)$_2$]$_3$(THF) (0.051 g, 0.091 mmol). ^{1}H NMR (500 MHz, C_6D_6, 313 K): δ 0.45 (d, $^3J_{H-H}$ = 2.8 Hz, 12H, SiH(CH_3)$_2$), 1.29 (m, 4H, α-CH_2 THF), 1.72 (s, 6H, C(CH_3)$_2$), 2.15 (s, 6H, C(CH_3)$_2$), 2.29 (t, $^3J_{H-H}$ = 5.2 Hz, 2H, NCH_2CH$_2$OCH$_3$), 2.35 (s, 6H, ArCH_3), 2.73–2.80 (m, 7H, NCH$_2$CH$_2$OCH_3 + ArCH_2 + NCH$_2$CH_2OCH$_3$), 3.14 (br s, 4H, β-CH_2 THF), 3.62 (br s, 2H, ArCH_2), 4.77 (m, 2H, Si*H*(CH$_3$)$_2$), 6.76 (s, 2H, Haro), 6.94 (t, J_{H-H} = 7.3 Hz, 2H, Haro), 7.09 (t, J_{H-H} = 7.5 Hz, 4H, Haro), 7.29 (m, 2H, Haro), 7.37 (d, J_{H-H} = 8.0 Hz, 4H, Haro). ^{13}C{^{1}H} NMR (125 MHz, C_6D_6, 313 K): δ 4.2 (SiH(*C*H$_3$)$_2$), 20.7 (ArCH_3), 24.8 (α-*C*H$_2$ THF), 27.7 (C(*C*H$_3$)$_2$), 33.0 (C(*C*H$_3$)$_2$), 42.7 (*C*(CH$_3$)$_2$), 48.2 (N*C*H$_2$CH$_2$OCH$_3$), 59.5 (Ar*C*H$_2$), 63.9 (NCH$_2$*C*H$_2$OCH$_3$), 69.9 (β-*C*H$_2$ THF), 72.9 (NCH$_2$CH$_2$O*C*H$_3$), 122.1 (aryl-*C*q), 124.2 (aryl-*C*H), 124.3 (aryl-*C*q), 126.4 (aryl-*C*H), 127.4 (aryl-*C*H), 128.9 (aryl-*C*H), 129.9 (aryl-*C*H), 136.5 (aryl-*C*q), 152.9 (aryl-*C*q), 161.4 (aryl-*C*q). ^{29}Si{^{1}H} NMR (79 MHz, C_6D_6, 313 K): δ −23.3 (s). ^{29}Si NMR (79 MHz, C_6D_6, 313 K): δ −23.3 (d of multiplets, $^1J_{Si-H}$ = 172 Hz).

NMR-scale generation of Y{ONOO^{CumCl,Me}}(N(SiHMe$_2$)$_2$) (Y-3). This product was prepared *in situ* as described above for **Y-1**, starting from {ONOO^{CumCl,Me}}H_2 (0.100 g, 0.161 mmol) and Y[N(SiHMe$_2$)$_2$]$_3$(THF) (0.090 g, 0.161 mmol). ^{1}H NMR (400 MHz, C_6D_6, 333 K): δ 0.37 (d, $^3J_{H-H}$ = 2.8 Hz, 12H, SiH(CH_3)$_2$), 1.36 (m, 4H, α-CH_2 THF), 1.60 (s, 6H, C(CH_3)$_2$), 2.03 (s, 6H, C(CH_3)$_2$), 2.26 (t, $^3J_{H-H}$ = 5.4 Hz, 2H, ArCH_2), 2.33 (s, 6H, ArCH_3), 2.73–2.76 (m, 5H, NCH$_2$CH_2OCH_3 + ArCH_2 + NCH_2CH$_2$OCH_3), 3.07 (br s, 4H, β-CH_2 THF), 3.56 (d, 2H, $^3J_{H-H}$ = 12.3 Hz, NCH$_2$CH_2OCH$_3$), 4.68–4.69 (m, 2H, Si*H*(CH$_3$)$_2$), 6.73 (s, 2H, Haro), 7.05 (s, 2H, Haro), 7.07 (s, 2H, Haro), 7.14 (s, 4H, Haro), 7.24 (s, 2H, Haro). ^{13}C{^{1}H} NMR (100 MHz, C_6D_6, 333 K): δ 4.1 (SiH(*C*H$_3$)$_2$), 20.6 (ArCH_3), 24.7 (α-*C*H$_2$ THF), 27.6 (C(*C*H$_3$)$_2$), 32.7 (C(*C*H$_3$)$_2$), 41.9 (*C*(CH$_3$)$_2$), 48.3 (Ar*C*H$_2$), 59.7 (Ar*C*H$_3$), 63.6 (NCH$_2$*C*H$_2$OCH$_3$), 70.3 (β-*C*H$_2$ THF), 72.7 (NCH$_2$CH$_2$O*C*H$_3$), 122.3 (aryl-*C*q), 124.3 (aryl-*C*q), 127.4 (aryl-*C*q), 127.5 (aryl-*C*H), 127.8 (aryl-*C*H), 128.6 (aryl-*C*H), 130.0 (aryl-*C*H), 135.9 (aryl-*C*q), 151.5 (aryl-*C*q), 161.2 (aryl-*C*q). ^{29}Si{^{1}H} NMR (79 MHz, C_6D_6, 333 K): δ −23.27 (s). ^{29}Si NMR (79 MHz, C_6D_6, 333 K): δ −23.3 (d of multiplets, $^1J_{Si-H}$ = 173 Hz, $^2J_{Si-H}$ = 6.3 Hz).

General procedure for polymerization of *rac*-lactide

In a typical experiment, in a glovebox, a Schlenk flask was charged with a solution of complex **Sc-1** (10.0 mg, 13.5 μmol) in toluene (1.0 mL). To this solution, *rac*-lactide (0.195 g, 1.35 mmol, 100 equiv. *vs*. Sc) was added rapidly. The mixture was immediately stirred with a magnetic stirrer bar at 60 °C for 1 h. An aliquot of the crude material was periodically sampled by pipette for determining monomer conversion by ^{1}H NMR spectroscopy. *Rac*-LA conversions were calculated from ^{1}H NMR spectra of the crude reaction mixtures in $CDCl_3$, from the integration (Int.) ratio Int.$_{polymer}$/[Int.$_{polymer}$ + Int.$_{monomer}$], using the methyl hydrogen resonances for PLA at δ 1.49 ppm and for LA at δ 1.16 ppm. The reaction was quenched by adding acidic methanol (*ca*. 1 mL of a 1.2 M HCl solution in MeOH), and the polymer was precipitated with an excess amount of methanol (*ca*. 100 mL). The polymer was then filtered and dried under vacuum to a constant weight. The microstructure of PLAs was determined by homodecoupling ^{1}H NMR spectroscopy (methine region) at 20 °C in $CDCl_3$ on a Bruker AC-500 spectrometer.

General procedure for polymerization of *rac*-β-butyrolactone

In a typical experiment, in the glovebox, a Schlenk flask was charged with a ligand {ONNO^{Cum,Me}}H_2 (6.64 mg, 11.7 μmol) and Y[N(SiHMe$_2$)$_2$]$_3$(THF) (6.56 mg, 11.7 μmol). Toluene (0.5 mL) was added at room temperature and the reaction mixture was stirred for 10 min at 20 °C. To this solution, *rac*-β-butyrolactone (0.101 g, 1.17 mmol, 100 equiv. *vs*. Y) was added rapidly. The mixture was immediately stirred with a magnetic stirrer bar at 20 °C for 2 min. The reaction was processed and worked-up similarly to that described above for lactide polymerization. Monomer (BL) conversions were calculated from ^{1}H NMR spectra of the crude reaction mixtures in $CDCl_3$, from the integration (Int.) ratio Int.$_{polymer}$/[Int.$_{polymer}$ + Int.$_{monomer}$], using the methylene hydrogen resonances for PHB at δ 1.49 ppm and for *rac*-BL at δ 1.16 ppm. The microstructure of PHBs was determined by ^{13}C NMR spectroscopy (methylene region) at 20 °C in $CDCl_3$ on a Bruker AM-500 spectrometer.

Single crystal X-ray diffraction studies

Diffraction data for pro-ligands **L1**, **L2**, **L3** and complexes **Sc-1**, **Sc-3**, **Sc-4**, and **Y-2** were collected at 100(2) K using a Bruker APEX CCD diffractometer with graphite-monochromatized $Mo_{K\alpha}$ radiation (λ = 0.71073 Å). A combination of ω and ϕ scans was carried out to obtain at least a unique data set. The crystal structures were solved by direct methods, the remaining atoms were located from difference Fourier synthesis followed by full-matrix least-squares refinement based on F^2 (programs SIR97 and SHELXL-97)[19] with the aid of the WINGX program.[20] In most cases, many hydrogen atoms could be found from the Fourier difference analysis. Other hydrogen atoms were placed at calculated positions and forced to ride on the attached atom. The hydrogen atom contributions were calculated but not refined. All non-hydrogen atoms were refined with anisotropic displacement parameters. The locations of the largest peaks in the final difference Fourier map calculation as well as the magnitude of the residual electron densities were of no chemical significance. Crystal data and details of data collection and structure refinement for pro-ligands **L1**, **L2**, and **L3** and complexes **Sc-1**, **Sc-3**, **Sc-4**, and **Y-2** are summarized in Tables S2–S4.†

Acknowledgements

This work was supported in part by the Ministère de l'Enseignement Supérieur et de la Recherche, CNRS, CAPES-COFECUB joined action Ph556-07_2007-2010 and CAPES-CNRS joined action PICS05923. We thank S. Sinbandhit (University of Rennes 1) for NMR experiments.

Notes and references

1 For leading reviews, see: (*a*) B. J. O'Keefe, M. A. Hillmyer and W. B. Tolman, *J. Chem. Soc., Dalton Trans.*, 2001, 2215; (*b*) O. Dechy-Cabaret, B. Martin-Vaca and D. Bourissou, *Chem. Rev.*, 2004, **104**, 6147; (*c*) C. K. Williams and M. A. Hillmyer, *Polym. Rev.*, 2008, **48**, 1; (*d*) C. M. Thomas, *Chem. Soc. Rev.*, 2010, **39**, 165; (*e*) M. J. Stanford and A. P. Dove, *Chem. Soc. Rev.*, 2010, **39**, 486; (*f*) J.-F. Carpentier, *Macromol. Rapid Commun.*, 2010, **31**, 1696; (*g*) N. Ajellal, J.-F. Carpentier, C. Guillaume, S. M. Guillaume, M. Helou, V. Poirier, Y. Sarazin and A. Trifonov, *Dalton Trans.*, 2010, **39**, 8363; (*h*) P. J. Dijkstra, H. Du and J. Feijen, *Polym. Chem.*, 2011, **2**, 520; (*i*) J.-C. Buffet and J. Okuda, *Polym. Chem.*, 2011, **2**, 2758.

2 For pioneering work in this field, see: (*a*) S. J. McClain, T. M. Ford and N. E. Drysdale, *Polym. Prepr. (Am. Chem. Soc., Div. Polym. Chem.)*, 1992, 463; (*b*) A. Le Borgne, C. Pluta and N. Spassky, *Macromol. Rapid Commmun.*, 1994, **15**, 955; (*c*) W. M. Stevels, M. J. K. Ankone, P. J. Dijkstra and J. Feijen, *Macromol. Chem. Phys.*, 1995, **196**, 1153; (*d*) V. Simic, N. Spassky and L. G. Hubert-Pfalzgraf, *Macromolecules*, 1997, **30**, 7338; (*e*) B. M. Chamberlain, Y. Sun, J. R. Hagadorn, E. W. Hemmesch, V. G. Young Jr., M. Pink, M. A. Hillmyer and W. B. Tolman, *Macromolecules*, 1999, **32**, 2400; (*f*) B. M. Chamberlain, B. A. Jazdzewski, M. Pink, M. A. Hillmyer and W. B. Tolman, *Macromolecules*, 2000, **33**, 3970; (*g*) T. M. Ovitt and G. W. Coates, *J. Am. Chem. Soc.*, 2002, **124**, 1316.

3 (*a*) C.-X. Cai, A. Amgoune, C. W. Lehmann and J.-F. Carpentier, *Chem. Commun.*, 2004, 330; (*b*) A. Amgoune, C. M. Thomas, T. Roisnel and J.-F. Carpentier, *Chem. – Eur. J.*, 2006, **12**, 169; (*c*) X. Liu, X. Shang, T. Tang, N. Hu, F. Pei, D. Cui, X. Chen and X. Jing, *Organometallics*, 2007, **26**, 2747; (*d*) H. E. Dyer, S. Huijser, N. Susperregui, F. Bonnet, A. D. Schwarz, R. Duchateau, L. Maron and P. Mountford, *Organometallics*, 2010, **29**, 3602; (*e*) L. Clark, M. G. Cushion, H. E. Dyer, A. D. Schwarz, R. Duchateau and P. Mountford, *Chem. Commun.*, 2010, **46**, 273; (*f*) W. Zhao, D. Cui, X. Liu and X. Chen, *Macromolecules*, 2010, **43**, 6678; (*g*) K. Nie, X. Gu, Y. Yao, Y. Zhang and Q. Shen, *Dalton Trans.*, 2010, **39**, 6832; (*h*) K. Nie, L. Fang, Y. Yao, Y. Zhang, Q. Shen and Y. Wang, *Inorg. Chem.*, 2012, **51**, 11133.

4 (*a*) A. Amgoune, C. M. Thomas, S. Ilinca, T. Roisnel and J.-F. Carpentier, *Angew. Chem., Int. Ed.*, 2006, **45**, 2782; (*b*) N. Ajellal, M. Bouyahyi, A. Amgoune, C. M. Thomas, A. Bondon, I. Pillin, Y. Grohens and J.-F. Carpentier, *Macromolecules*, 2009, **42**, 987; (*c*) M. Bouyahyi, N. Ajellal, E. Kirillov, C. M. Thomas and J. F. Carpentier, *Chem. – Eur. J.*, 2011, **17**, 1872; (*d*) C. G. Jaffredo, Y. Chapurina, S. M. Guillaume and J.-F. Carpentier, *Angew. Chem., Int. Ed.*, 2014, **53**, 2687.

5 For the valuable use of cumyl substituents in ROP, see also: (*a*) H.-L. Chen, S. Dutta, P.-Y. Huang and C.-C. Lin, *Organometallics*, 2012, **31**, 2016; (*b*) L. Wang and H. Ma, *Macromolecules*, 2010, **43**, 6535; see also ref. 9*b*. Note, however, that this trend may not necessarily be true with some specific substrates, such as β-malolactonates; see ref. 4*d*.

6 For selected references evidencing superiority of small rare earth metal centers in achieving highly selective ROP reactions, see: (*a*) H. Ma, T. P. Spaniol and J. Okuda, *Inorg. Chem.*, 2008, **47**, 3328; (*b*) H. E. Dyer, S. Huijser, A. D. Schwarz, C. Wang, R. Duchateau and P. Mountford, *Dalton Trans.*, 2008, 32; (*c*) L. M. Hodgson, R. H. Platel, A. J. P. White and C. K. Williams, *Macromolecules*, 2008, **41**, 8603; (*d*) N. Ajellal, D. M. Lyubov, M. A. Sinenkov, G. K. Fukin, A. V. Cherkasov, C. M. Thomas, J.-F. Carpentier and A. A. Trifonov, *Chem. – Eur. J.*, 2008, **14**, 5440; (*e*) R. H. Platel, A. J. P. White and C. K. Williams, *Chem. Commun.*, 2009, 4115; (*f*) E. Grunova, E. Kirillov, T. Roisnel and J.-F. Carpentier, *Dalton Trans.*, 2010, **39**, 6739; (*g*) J. W. Kramer, D. S. Treiter, E. W. Dunn, P. M. Castro, T. Roisnel, C. M. Thomas and G. W. Coates, *J. Am. Chem. Soc.*, 2009, **131**, 16042; (*h*) R. H. Platel, A. J. P. White and C. K. Williams, *Inorg. Chem.*, 2011, **50**, 7718; (*i*) Z. C. Zhang and D. M. Cui, *Chem. – Eur. J.*, 2011, **17**, 11520; (*j*) G. Li, M. Lamberti, M. Mazzeo, D. Pappalardo, G. Roviello and C. Pellecchia, *Organometal-*

lics, 2012, **31**, 1180; (*k*) C. Bakewell, T.-P.-A. Cao, N. J. Long, X. F. Le Goff, A. Auffrant and C. K. Williams, *J. Am. Chem. Soc.*, 2012, **134**, 20577; (*l*) K. Nie, W. Gu, Y. Yao, Y. Zhang and Q. Shen, *Organometallics*, 2013, **32**, 2608; (*m*) C. Bakewell, T.-P.-A. Cao, X. F. Le Goff, N. J. Long, A. Auffrant and C. K. Williams, *Organometallics*, 2013, **32**, 1475; (*n*) D. Pappalardo, M. Bruno, M. Lamberti and C. Pellecchia, *Macromol. Chem. Phys.*, 2013, **214**, 1965; (*o*) M. Mazzeo, R. Tramontano, M. Lamberti, A. Pilone, S. Milione and C. Pellecchia, *Dalton Trans.*, 2013, **42**, 9338.

7 Ionic radius for 6-coordinate metals: Sc^{3+} = 0.745 Å, Y^{3+} = 0.90 Å, Lu^{3+} = 0.841 Å; R. D. Shannon, *Acta Crystallogr., Sect. A: Cryst. Phys., Diffr., Theor. Gen. Cryst.*, 1976, **32**, 751.

8 (*a*) M. E. G. Skinner, T. Toupence, B. R. Tyrrell, B. D. Ward, C. R. Wilson, A. R. Cowley and P. Mountford, *J. Organomet. Chem.*, 2002, **647**, 145; (*b*) C. L. Boyd, B. R. Tyrrell, B. D. Ward and P. Mountford, *Organometallics*, 2005, **24**, 309.

9 (*a*) H. Ma, T. P. Spaniol and J. Okuda, *Angew. Chem., Int. Ed.*, 2006, **45**, 7818; (*b*) J.-C. Buffet, A. Kapelski and J. Okuda, *Macromolecules*, 2010, **43**, 10201; (*c*) J.-C. Buffet and J. Okuda, *Dalton Trans.*, 2011, **40**, 7748; (*d*) A. Kapelski, J.-C. Buffet, T. P. Spaniol and J. Okuda, *Chem. – Asian J.*, 2012, **7**, 1320.

10 A. W. Addison, T. N. Rao, J. Reedijk, J. Van Rijn and G. C. Verschoor, *J. Chem. Soc., Dalton Trans.*, 1984, 1349–1356.

11 For examples of 5-coordinate Sc-bis(phenolate) complexes (yet structurally uncharacterized in the solid state), see ref. 6*n*.

12 J. Eppinger, M. Spiegler, W. Hieringer, W. A. Herrmann and R. Anwander, *J. Am. Chem. Soc.*, 2000, **122**, 3080.

13 (*a*) H. Ma, T. P. Spaniol and J. Okuda, *Dalton Trans.*, 2003, 4770; (*b*) M. Mazzeo, M. Lamberti, I. D'Auria, S. Milione, J. C. Petrers and C. Pellecchia, *J. Polym. Sci., Part A: Polym. Chem.*, 2010, **48**, 1374.

14 As earlier proposed for this class of catalysts and many other yttrium amide complexes (ref. 3), the relatively high PDI values observed are likely due to the moderate initiation rate (as compared to propagation) of the amide group. The Y-isopropoxides are much better initiators. There is no evidence for aggregation of the yttrium amide precursors, nor of the active, propagating yttrium species; this has been demonstrated by recent studies on model *O*-lactate and β-alkoxy-butyrate yttrium complexes supported by bis(phenolate)-type ligands, which all proved to be mononuclear in solution and in the solid state; see: (*a*) J. S. Klitzke, T. Roisnel, E. Kirillov, O. de L. Casagrande Jr. and J.-F. Carpentier, *Organometallics*, 2014, **33**, 309; (*b*) J. S. Klitzke, T. Roisnel, E. Kirillov, O. de L. Casagrande Jr. and J.-F. Carpentier, *Organometallics*, 2014, DOI: 10.1021/om401214q, in press.

15 ROP of *rac*-BL was performed at 2.4 M, since a high monomer concentration was previously noted to be a key parameter for achieving high activities in ROP of such β-lactones; see ref. 4*a*–*c*. A direct comparison with ROP of *rac*-LA was not possible, since this less soluble monomer cannot be loaded at such high concentrations. At 1.0 M monomer concentration, ROP of *rac*-LA with yttrium catalysts of the type **Y-1**–**Y-4** proceeded significantly faster than ROP of *rac*-BL.

16 (*a*) K. C. Hultzsch, P. Voth, K. Beckerle, T. P. Spaniol and J. Okuda, *Organometallics*, 2000, **19**, 228; (*b*) R. Anwander, O. Runte, G. Eppinder, G. Gerstberger, E. Herdtweek and M. Spiegler, *Dalton Trans.*, 1998, 847.

17 A. Kowalski, A. Duda and S. Penczek, *Macromolecules*, 1998, **31**, 2114.

18 A. I. Kochnev, I. I. Oleynik, I. V. Oleynik, S. S. Ivanchev and G. A. Tolstikov, *Russ. Chem. Bull., Int. Ed.*, 2007, **56**, 1125.

19 (*a*) A. Altomare, M. C. Burla, M. Camalli, G. Cascarano, C. Giacovazzo, A. Guagliardi, A. G. G. Moliterni, G. Polidori and R. Spagna, *J. Appl. Crystallogr.*, 1999, **32**, 115; (*b*) G. M. Sheldrick, *SHELXS-97, Program for the Determination of Crystal Structures*, University of Goettingen, Germany, 1997; (*c*) G. M. Sheldrick, *SHELXL-97, Program for the Refinement of Crystal Structures*, University of Goettingen, Germany, 1997; (*d*) G. M. Sheldrick, *Acta Crystallogr.*, 2008, **64**, 112.

20 L. J. Farrugia, *J. Appl. Crystallogr.*, 1999, **32**, 837.

